2014-05-24

Plant degreening: evolution and expression of tomato (Solanum lycopersicum) dephytylation enzymes

Gene, Amsterdam, v.546, n.2, p.359-366, 2014
http://www.producao.usp.br/handle/BDPI/45244

Gene 546 (2014) 359–366

Contents lists available at ScienceDirect

Gene

journal homepage: www.elsevier.com/locate/gene

Plant degreening: evolution and expression of tomato (*Solanum lycopersicum*) dephytylation enzymes

Bruno Silvestre Lira [a], Nathalia de Setta [b], Daniele Rosado [a], Juliana Almeida [a], Luciano Freschi [a], Magdalena Rossi [a,*]

[a] Departamento de Botânica, Instituto de Biociências, Universidade de São Paulo, São Paulo, SP, Brazil
[b] Centro de Ciências Naturais e Humanas, Universidade Federal do ABC, Santo André, SP, Brazil

ARTICLE INFO

Article history:
Received 5 November 2013
Received in revised form 21 May 2014
Accepted 22 May 2014
Available online 24 May 2014

Keywords:
Chlorophyllase
Pheophytinase
Senescence
Ripening
Tomato

ABSTRACT

Chlorophyll is the most abundant pigment on earth and even though it is known that its high photo-excitability necessitates a tight regulation of its degradation pathway, to date there are still several steps in chlorophyll breakdown that remain obscure. In order to better understand the 'degreening' processes that accompany leaf senescence and fruit ripening, we characterized the enzyme-encoding genes involved in dephytylation from tomato (*Solanum lycopersicum*). A single pheophytinase (*PPH*) gene and four chlorophyllase (*CLH*) genes were identified in the tomato genome. A phenetic analysis revealed two groups of CLHs in eudicot species and further evolutionary analysis indicated that these enzymes are under diverse selection pressures. A comprehensive expression profile analysis also suggested functional specificity for these dephytylating enzymes. The integrated analysis allows us to propose three general roles for chlorophyll dephytylation: *i*) PPH, which is under high selective constraint, is responsible for chlorophyll degradation during developmentally programed physiological processes; *ii*) Group I CLHs, which are under relaxed selection constraint, respond to environmental and hormonal stimuli and play a role in plant adaptation plasticity; and *iii*) Group II CLHs, which are also under high selective constraint, are mostly involved in chlorophyll recycling.

1. Introduction

Chlorophyll (Chl) is responsible for light absorption during photosynthesis, a process upon which life on Earth depends. Chl is composed of a tetrapyrrole ring with a central magnesium ion and a phytol chain and its metabolism can be divided into three phases: biosynthesis, the chlorophyll cycle, and degradation. However, in part due to its complex biochemical structure, various aspects of Chl metabolism are still poorly understood, and this is especially true for those associated with its degradation (Hörtensteiner, 2013). In general, the Chl degradation pathway resembles bacterial detoxification processes, and for many years it was considered to be a simple Chl detoxification phenomenon (Hörtensteiner, 2006). However, recent studies indicate that the process is more complicated since more Chl derived catabolites are being discovered, although few of these have been assigned a biological function (Hörtensteiner, 2013; Hörtensteiner and Kräutler, 2011).

Chl breakdown sequentially involves a dephytylation step, tetrapyrrole ring opening and catabolite inactivation to avoid phototoxicity of Chl degradation products, resulting in a linear tetrapyrrole molecule that is stored in the vacuole. For many years, it was accepted that dephytylation was catalyzed by chlorophyllase (CLH), an enzyme that hydrolyzes Chl *a* to generate phytol and chlorophyllide (Chlide *a*), a compound that is further converted to pheophorbide *a* (Pheide *a*) by a still unknown metal dechelatase. The enzyme pheophorbide *a* oxygenase (PAO) then opens the tetrapyrrolic backbone structure, producing the red chlorophyll catabolite (RCC) that follows the "PAO pathway" of Chl breakdown until catabolite inactivation (Hörtensteiner, 2013). However, data obtained from experiments with *Arabidopsis thaliana* double mutants demonstrated that CLHs are not required for senescence-related Chl breakdown in vivo (Schenk et al., 2007). Furthermore, subcellular localization analyses have resulted in contradicting observations since *Arabidopsis* CLHs have been reported to be cytoplasmic proteins (Schenk et al., 2007), while it was demonstrated that a *Citrus* CLH resides in the plastid and is post-transcriptionally

Abbreviations: ABA, abscisic acid; Chl, chlorophyll; Chlide, chlorophyllide; CLH, chlorophyllase; *dN*, non-synonymous distance; *dS*, synonymous distance; *gf*, green flesh mutant; LTR, likelihood ratio test; MS, Murashige and Skoog media; Nc, number of codons; PAO, pheophorbide a oxygenase; PAR, photosynthetically active radiation; pFCC, primary fluorescent chlorophyll catabolite; Pheide, pheophorbide; Pheo, pheophytin; PPH, pheophytinase; RCC, red chlorophyll catabolite; SAG12, senescence associated gene 12; SE, standard error; SGR, stay green protein; UTR, untranslated regions.

* Corresponding author at: Departamento de Botânica, Instituto de Biociências, Universidade de São Paulo, Rua do Matão, 277, 05508-900 São Paulo, Brazil.
E-mail addresses: bslbsl@usp.br (B.S. Lira), setta@ufabc.edu.br (N. de Setta), daniele.rosado@usp.br (D. Rosado), juliana.almeida.silva@usp.br (J. Almeida), freschi@usp.br (L. Freschi), mmrossi@usp.br (M. Rossi).

http://dx.doi.org/10.1016/j.gene.2014.05.051
0378-1119/

regulated by cleavage (Azoulay-Shemer et al., 2008, 2011; Harpaz-Saad et al., 2007). This discrepancy might reflect a difference in experimental approaches, but this issue remains to be resolved. In 2009, Schelbert et al. identified an *A. thaliana* plastidial protein that dephytylates the Mg-free Chl *a*, pheophytin (Pheo *a*), yielding phytol and Pheide *a*. This new dephytylating enzyme was named pheophytinase (PPH) and shown to be associated with the thylakoid membrane as part of a Chl breakdown complex recruited by the STAY-GREEN protein (SGR). Interestingly, this degradation complex involves all the enzymes that catalyze the stepwise degradation of Chl to the compound known as primary fluorescent chlorophyll catabolite (pFCC), allowing metabolic channeling of phototoxic Chl breakdown intermediates. Subsequently, pFCC is exported from the plastid to the vacuole (Sakuraba et al., 2013). Interestingly, CLH is not part of this enzymatic complex (Sakuraba et al., 2012), suggesting different and/or complementary roles for the two dephytylation enzymes.

Chl degradation has been extensively investigated and most studies to date have used leaf senescence as the associated experimental system. Leaf senescence is a highly regulated process that involves several changes in cell structure, metabolism, and gene expression. The earliest and most evident cell structure change is the breakdown of the chloroplast, accompanied by catabolism of chlorophyll and macromolecules (e.g. proteins, lipids, and RNA). Regarding gene expression, leaf senescence is characterized by the decrease of genes related to photosynthesis and protein synthesis and by increased expression of senescence-associated genes (SAGs) (Lim et al., 2007). Senescence is an integrated response of plants to endogenous developmental and external environmental stimuli, and plant hormones play an important role in signaling. Our current understanding of the relationship between environmental responses and leaf senescence comes from the study of senescence response to the phytohormone abscisic acid (ABA), involved in response to abiotic stresses such as drought, high salt condition, and low temperature and; jasmonic acid (JA) and salicylic acid (SA) that participate in biotic stress regulation. Meanwhile, ethylene has extensively been described as a major hormone in hastening age-dependent leaf senescence (Khan et al., 2013). However, relatively little is known about other examples when degreening occurs, such as the mechanisms of Chl degradation that accompany fruit ripening (Hörtensteiner, 2013). Fleshy fruit ripening involves major biochemical and physiological alterations that influence texture, flavor and aroma as well as color (Seymour et al., 2013). This complex metabolic process is mainly controlled by ABA and ethylene. In the climacteric fruits such as tomato, there is an increase in ABA preceding the increase in ethylene. Exogenous application of ABA induces ethylene through the transcriptional activation of the biosynthesis genes, while the suppression of ABA leads to a delay in fruit ripening (McAtee et al., 2013). Additionally, this hormone has also been associated with fruit growth in tomato. ABA accumulates at the end of the expansion phase, and ABA-deficient mutants have reduced fruit size (Nitsch et al., 2012). In this framework, the cultivated tomato, *Solanum lycopersicum*, whose fruit exhibits clear color changes during maturation, is a potentially valuable model for comparative studies of degreening during leaf senescence and fruit ripening in relationship with their hormonal control. To our knowledge, the only report describing Chl degradation-associated genes in *S. lycopersicum* (Efrati et al., 2005) involved the mapping of three *CLH* genes and a *PAO* gene as part of a search for candidates for the *gf* (*green flesh*) mutant phenotype, which was later demonstrated to be SGR (Barry et al., 2008).

In this current study, we performed a genomic and evolutionary characterization of tomato *CLH* and *PPH* genes, in order to gain a more comprehensive understanding of their role in Chl dephytylation. Additionally, the expression patterns of these genes in leaves submitted to different hormonal treatments and during fruit development and ripening were analyzed. Our data demonstrate that the diversity of dephytylating enzymes is associated with different selective constraints and expression profiles, suggesting functional specialization.

2. Materials and methods

2.1. Phenetic and evolutionary analyses

Tomato *CLH* and *PPH* gene sequences were identified by using the coding sequence of both *A. thaliana CLH* genes (AT1G19670 and AT5G43860) and the *PPH* gene (AT5G13800) to interrogate the tomato genome sequence, available at the Sol Genomics Network (http://solgenomics.net/). The chromosomal locations were determined by the position of the closest marker, based on the Tomato-EXPEN-2000 map (http://solgenomics.net/). In silico prediction of the protein subcellular localization was performed using TargetP (Emanuelsson et al., 2007), Cello v2.5 (Yu et al., 2006), SherLoc2 (Briesemeister et al., 2009), MultiLoc2 (Blum et al., 2009), BaCelLo (Pierleoni et al., 2006), Plant-mPLoc (Chou and Shen, 2010), ChloroP (Emanuelsson et al., 2007) and iPSORT (Bannai et al., 2002). Other plant sequences that are homologous to the *A. thaliana CLHs* and *PPH* genes were identified by searching the Phytozome 9.0 database (http://www.phytozome.net/), NCBI (http://www.ncbi.nlm.nih.gov) and Sol Genomics Network, using the tBLASTx program (Altschul et al., 1990). The sequences were aligned using the MUSCLE package available in the MEGA 5.2 software with default parameters (Tamura et al., 2007) in a codon-based manner and inspected manually. The alignment was analyzed using the Neighbor-Joining method, the distances were calculated according to the best model pointed by MEGA 5.2 software and the tree topology was evaluated with 5000 bootstrap replications. Detailed information of all sequences used for the analyses is shown in Table S1.

The evolutionary analysis was performed as previously described by Almeida et al. (2011). Non-synonymous (*dN*) and synonymous (*dS*) distances, as well as their standard error (SE) values were estimated by the Nei–Gojobori method (p-distance) using the MEGA 5.2 software. In order to preserve the reading frames, the alignment gaps were deleted. Alignments are presented in Figs. S1 to S10. Codon bias was determined by the effective number of codons (Nc) value computed by the CodonW program (mobyle.pasteur.fr/cgi-bin/portal.py?-form¼codonw). The Nc value varies from 21, when only one codon is used per amino acid, to 61, when synonymous codons for each amino acid are used at similar frequencies. One-way ANOVA with Tukey's posthoc test was performed using the InfoStat software (www.infostat.com, Grupo InfoStat, FCA, Universidad Nacional de Córdoba, Argentina) to evaluate significant differences in codon usage. In order to compare codon evolution models to determine selective constraint, three models were fitted using the CODEML program of the PAML suite (Yang, 2007). The first model, M0, assumes that all codons across the sequences have the same dN/dS ratio (ω). The value for ω provides an indication of the selection at the protein level: $0 < \omega < 1$ indicates purifying selection; $\omega = 1$ is neutral evolution; and $\omega > 1$ points to the presence of positive selection. Model M1a suggests the existence of two classes of codons, a proportion with $0 < \omega < 1$ and the remainder of codons with $\omega = 1$. Model M2a indicates three types of codon evolution: purifying selection, neutral evolution, and positive selection. The fit of models M0 versus M1a, and M1a versus M2a was evaluated by a likelihood ratio test (LRT), comparing the difference in log likelihoods with a χ^2 distribution two times (Yang, 2007).

2.2. Plant material

S. lycopersicum L. (cv. MicroTom) seeds were obtained from the Laboratory of Hormonal Control of Plant Development (ESALQ, Universidade de São Paulo). The plants were grown in 1 L pots in a greenhouse under automatic irrigation (four times a day) at an average mean temperature of 25 °C, 11.5 h/13 h (winter/summer) photoperiod and 250–350 μmol m^{-2} s^{-1} of incident photo-irradiance. Fruit pericarp material (without placenta and locule walls) at the green (G, ~1.5 cm in diameter), mature green (MG, jelly placenta and ~2.5 cm in diameter),

yellow (Y, ~2.5 cm in diameter) and ripe (R, ~2.5 cm in diameter) stages was harvested at 15, 25, 28 and 45 days after anthesis. For phytohormone-regulated senescence assay, tomato seeds were surface-sterilized according to Pino et al. (2010) and germinated on half strength MS salts (Murashige and Skoog, 1962), 30 g L^{-1} sucrose and 2 g L^{-1} Phytagel (Sigma, St. Louis, MO, USA). The growth chamber conditions were 400 μmol PAR m^{-2} s^{-1} with a 12 h photoperiod and air temperature of 25 ± 1 °C. Four-week-old in vitro plants were treated with 100 μM abscisic acid (ABA), 100 μM salicylic acid (SA) or 5 mL L^{-1} ethylene (ET). Treatment with 500 μL L^{-1} 1-methylcyclopropene (MCP), an inhibitor of ethylene perception (Blankenship and Dole, 2003), started three weeks before harvest time and was renewed weekly. Proper volumes of the gaseous ET and MCP solutions were added in the headspace of the sealed flasks containing the plants to achieve the final concentrations mentioned above. The preparation of MCP followed the manufacturer's instructions (SmartFresh® powder 0.14%). Source leaf tissue from the second node from the bottom of the plant was collected after two and four days of hormonal treatment. MCP-treated plants were harvested at the exact same age of those exposed to hormonal treatments. All samples were frozen in liquid nitrogen, powdered and stored at −80 °C.

2.3. Chlorophyll measurement

For chlorophyll *a* and *b* quantification, 50 mg of homogenized tissue was incubated with *N*,*N*-dimethylformamide at room temperature in darkness for 1 h, the supernatant was collected and the extraction was repeated one more time. The absorption spectrum of the combined supernatants at 647 and 664 was measured and the pigment content was calculated as described by Lichtenthaler (1987). Chlorophyll data were analyzed by ANOVA followed by a Tukey test ($p < 0.05$) using the Infostat software (Di Rienzo et al., 2011).

2.4. qPCR

RNA extraction and qPCR reactions were performed as described by Quadrana et al. (2013). The PCR primers used are listed in Table S2. The *SlPAO* (Solyc11g066440) and *SlSAG12* (Solyc02g076910) genes were

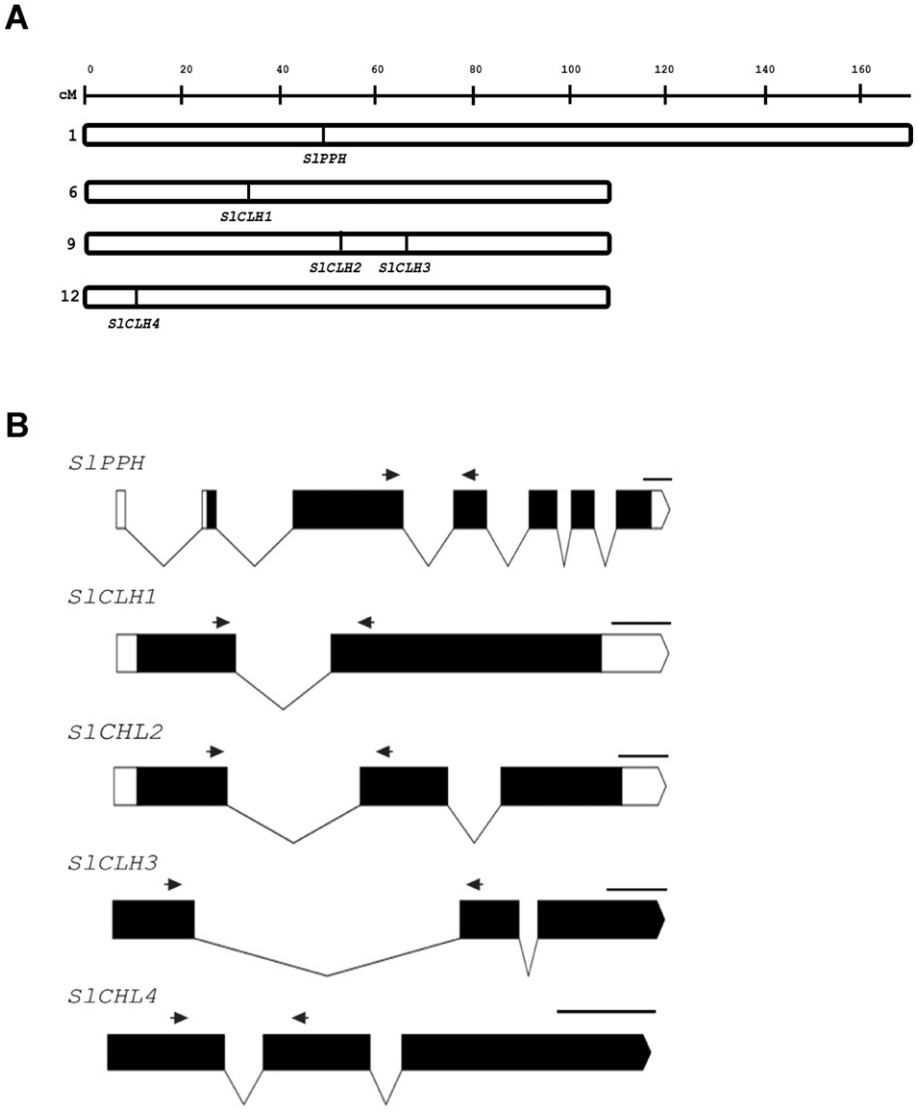

Fig. 1. Genomic characterization of *S. lycopersicum* chlorophyllase and pheophytinase genes. (A) Chromosomal positioning of SlCLH1 (Solyc06g053980.2), SlCLH2 (Solyc09g065620.2), SlCLH3 (Solyc09g082600.1), SlCLH4 (Solyc12g005300.1) and SlPPH (Solyc01g088090.1) according to the closest marker mapped onto the Tomato-EXPEN-2000 map (http://solgenomics.net/). T0834 (32 cM) for *SlCLH1*, C2_At4g02680 (56.3 cM) for *SlCLH2*, cLET-42-O2 (72 cM) for *SlCLH3*, TG180 (9 cM) for *SlCLH4* and T1677 (46 cM) for *SlPPH*. (B) Schematic representation of gene structures. Black boxes and lines indicate exons and introns, respectively. Untranslated regions (UTRs) are represented as white boxes for those genes with available information. The gray arrows represent the primers used for the qPCR experiments. Scale bar indicates 200 bp. The representation was made with Exon–Intron Graphic Maker (http://wormweb.org/exonintron).

used as controls for chlorophyll degradation and senescence related gene expression, respectively. All reactions were performed with two technical replicates and at least three biological replicates. mRNA levels were quantified using a 7500 Real-Time PCR system (Applied Biosystem) and SYBR Green Master Mix (Applied Biosystem). Data were analyzed with LinRegPCR software (Ruijter et al., 2009) to obtain Ct values and to calculate primer efficiency. Expression values were normalized to the mean of two constitutively expressed genes, TIP41 and Expressed (Quadrana et al., 2013). A permutation test, which lacks sample distribution assumptions (Pfaffl et al., 2002), was used to detect statistical ($p < 0.05$) differences in expression levels between samples and developmental stages using the algorithms in the fgStatistics software (Di Rienzo, 2009). The normalized expression pattern was presented by a heat map constructed with GENE-E program (http://www.broadinstitute.org/cancer/software/GENE-E/).

3. Results

3.1. Genomic and evolutionary characterization of PPH and CLHs

In order to evaluate the diversity of dephytylation enzymes, the tomato genome sequence (The Tomato Genome Consortium, 2012) was searched using *A. thaliana* CLHs and PPH coding sequences as queries. Four *CLH-like* and one *PPH-like* genes were identified, distributed on chromosomes 1, 6, 9 and 12 (Fig. 1A). These genes were named and will be referred to hereafter as *SlCLH1*, *SlCLH2*, *SlCLH3*, *SlCLH4*, and *SlPPH*. *SlPPH* contains seven exons and there is variation in the *SlCLH* gene structures, with two or three exons (Fig. 1B). In order to predict the subcellular location of tomato proteins, eight different programs were tested using the protein sequence of AtPPH as control, which is experimentally demonstrated to localize in chloroplasts (Schelbert et al., 2009). Interestingly, all tested programs accurately predicted AtPPH to be located in plastid. However, for tomato proteins the predictions were ambiguous. Most of the programs indicated that SlPPH is a plastidial protein whereas for SlCLHs suggested chloroplastic, cytosolic and even, plasma membrane localization (Table S3).

The topology of the *PPH* tree was for the most part in agreement with the phylogenetic distribution of the species and among the plant species considered, PPH was found to be mostly encoded by a single copy gene. When paralogs were found, as was the case for *Glycine max* and *Brassica rapa*, the sequences clustered together, indicating species-specific gene duplications (Fig. 2A).

The *CLH* phenetic analysis revealed one distinct clade containing all the Eudicot sequences, while those of the monocotyledonous species, conifers and *Eucaliptus grandis* grouped together in a not well supported clade (Fig. 2B). In agreement with that reported by Gupta et al. (2012), within the Eudicot clade, two groups could be distinguished, which are highlighted as Group I and Group II. All the analyzed species were represented by at least one *CLH* copy in each group, suggesting ancient gene duplication in the flowering plant lineage.

An integrated analysis of the phenogram, combined with the limited functional data available further revealed some interesting features. AtCLH1 (Benedetti et al., 1998; Liao et al., 2007; Tsuchiya et al., 1999), BoCLH1 (Büchert et al., 2011) and CsCLH3 (Jacob-Wilk et al., 1999), which belong to Group I, have been shown to be hormone or environmental stimuli-responsive enzymes; however, their paralogs are constitutively expressed, or suggested to be non-responsive to hormone treatments (Büchert et al., 2011; Tang et al., 2004).

The existence of two types of dephytylation enzymes in land plants, namely two paralog *CLH*-encoding genes and a single *PPH*, is intriguing in terms of their putative physiological roles as well as the evolutionary history of their functional differentiation. We therefore explored the patterns of sequence diversification by applying a likelihood ratio test (LRT) to evaluate the selective constraints in which these sequences are evolving. Three different models were tested. The first, M0, assumes that all codons have the same dN/dS (ω). The second, M1a, proposes

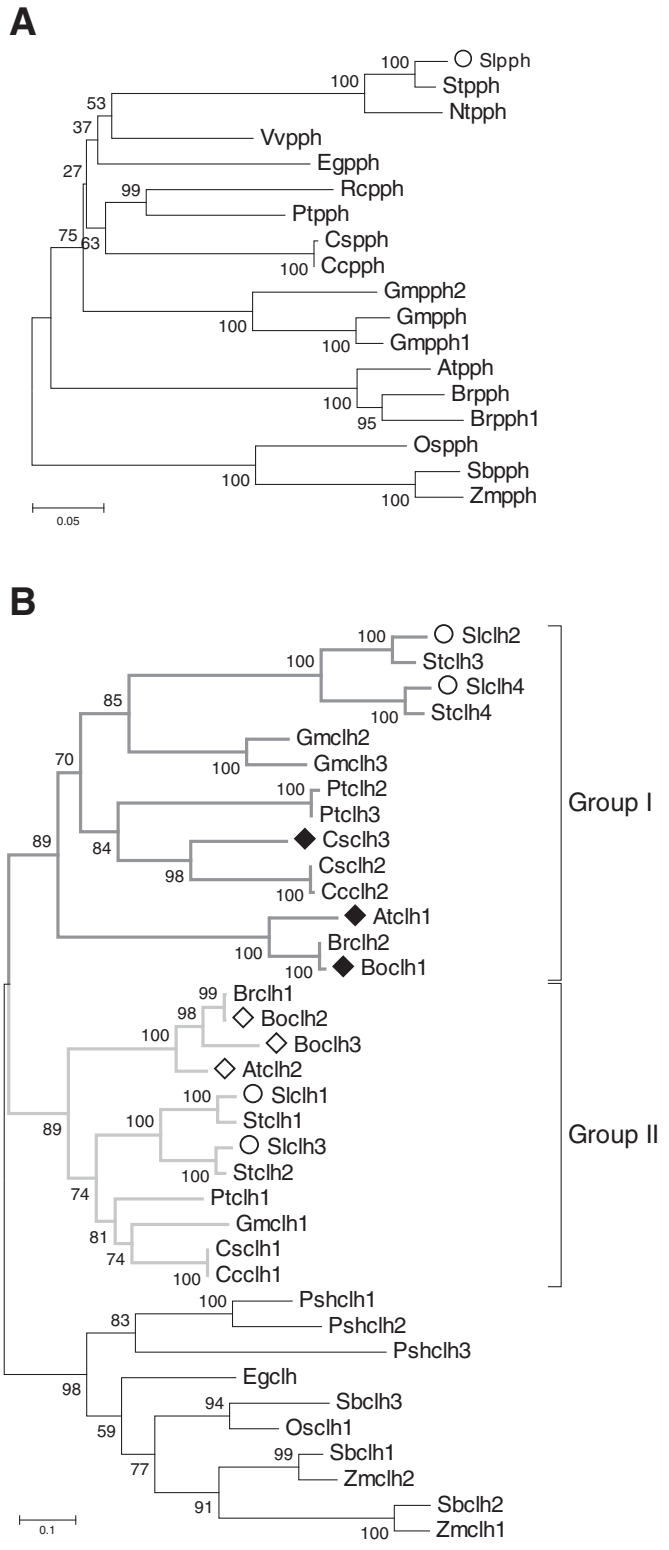

Fig. 2. Phenogram of *PPH*s and *CLH*s. Sequence diversity for *PPH*s (A) and *CLH*s (B). Details of sequence data are listed in Table S1. Only genes from species with fully sequenced genomes were included in the analysis. Within the Eudicots, two groups of *CLH*s, Groups I and II, could be distinguished. *S. lycopersicum* sequences are highlighted with open circles. Filled and open rhombuses indicate *CLH* sequences that have been functionally characterized as hormone-responsive or non-responsive, respectively. Bootstrap values are shown on the branches. *Arabidopsis thaliana* (At), *Brassica oleracea* (Bo), *Brassica rapa* (Br), *Citrus clementine* (Cc), *Citrus sinensis* (Cs), *Eucalyptus grandis* (Eg), *Glycine max* (Gm), *Nicotiana tabacum* (Nt), *Oryza sativa* (Os), *Picea sitchensis* (Ps), *Populus trichocarpa* (Pt), *Ricinus communis* (Rc), *Solanum lycopersicum* (Sl), *Solanum tuberosum* (St), *Sorghum bicolor* (Sb), *Vitis vinifera* (Vv), and *Zea mays* (Zm).

that a subset of codons is under purifying selection while the others exhibit neutral evolution. The third model, M2a, is able to categorize codons in three classes: those with purifying selection, those with a neutral evolution pattern, and the remainder that are under positive selection. In order to avoid data misinterpretation, the Nc was estimated and the comparison between species did not show statistically significant differences, indicating that there is no codon usage bias. No positive selection was detected for any of the groups of sequences tested (data not shown). When phylogenetically distant sequences were compared (all *PPH*s, all *CLH*s, Group I-*CLH*s or Group II-*CLH*s, Table 1), *PPH* and *CLH*s showed evidence of evolving in accordance with the M1a model, with both neutral and constrained evolving codons. However, looking exclusively at Solanaceae or Brassicaceae sequences, a different scenario was uncovered. While, *PPH* and Group II-*CLH*s have codons constrained exclusively by purifying selection, Group I-*CLH*s exhibited a relaxed selection, containing codons evolving by both purifying selection and neutral evolution (Table 1).

3.2. Expression profiles of tomato PPH and CLH genes upon hormone treatments and along fruit development and ripening

To generate additional evidence for an association between the roles of the different dephytylating enzymes with distinct physiological processes, we performed a comprehensive expression analysis in leaves submitted to different hormonal treatments and during fruit development and ripening (green (G), mature green (MG), yellow (Y) and ripe (R) stages). Chl *a* and Chl *b* levels decreased upon ET, ABA and SA treatments while the leaves grown in the presence of 1-methylcyclopropene (MCP), an inhibitor of ethylene perception, displayed higher levels of Chls (Fig. 3). As expected, Chl content also declined during ripening (Fig. 4). ET, ABA and SA treatments triggered leaf senescence as demonstrated by the increase of the mRNA levels of the *SlSAG12* gene, which is a senescence marker (Weaver et al., 1998). In MCP treated leaves, *SlSAG12* showed reduced amount of transcripts compared with control. *PAO* has shown to be ubiquitously expressed in green tissues to avoid the phototoxicity of Pheide *a* (Hörtensteiner, 2013). Thus, we might speculate that the increment in Chl content observed upon MCP treatment would result in increased levels of *PAO* mRNA as observed in Fig. 5 although, to our knowledge, this correlation is still unexplored. In agreement with previous report, *PAO* expression correlated positively with Chl degradation induced by ET, ABA and SA (Pružinska et al., 2003) (Fig. 5, Tables S4, S5).

Transcripts corresponding to the dephytylating enzymes SlCLH1, SlCLH4 and SlPPH were detected in all samples tested. *SlCLH2* showed expression in leaves, but only very low amounts of mRNA were detected in fruits and exclusively at the G stage. None of the analyzed samples

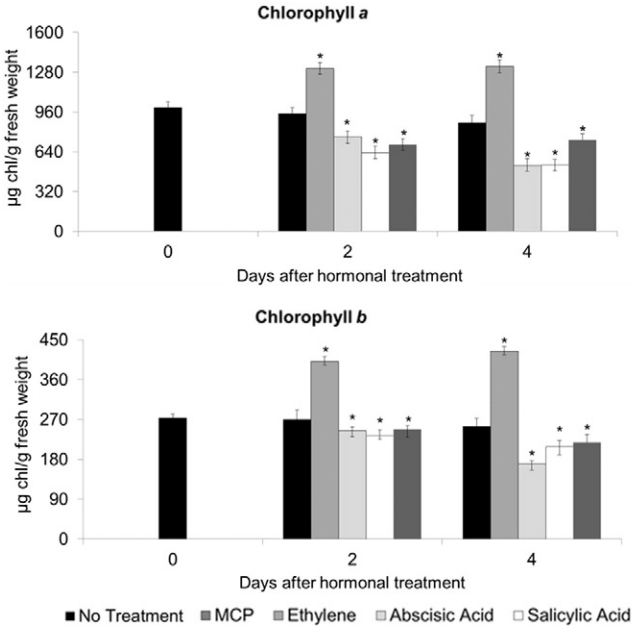

Fig. 3. Chlorophyll content upon hormonal treatment. Chlorophyll *a* and chlorophyll *b* content in leaves collected after 0, 2 and 4 days of hormonal treatment. MCP refers to 1-methylcyclopropene. Asterisks indicate statistically significant values compared with non-treated T0 ($p < 0.05$).

showed detectable levels of *SlCLH3* expression. In leaves *SlCLH2* and *SlCLH4* showed low and similar expression levels, which represent 4 and 8-fold less than *SlPPH* and *SlCLH1*, respectively. This difference in the magnitude of expression enlarges in fruits where *SlPPH* and *SlCLH1* displayed more than 50-fold mRNA than *SlCLH2* and *SlCLH4* (Table S6). A detailed analysis of the temporal and spatial expression patterns suggested that the four enzymes have distinct functional roles (Fig. 5, Table S4). *SlCLH1* expression correlated with Chl content showing a mild decrease following the three treatments that induced leaf senescence. In the presence of MCP, leaves maintained *SlCHL1* transcript level displaying a little reduction after 4 days. *SlCLH2* expression peaked after two days of MCP, ET and ABA treatment, while the presence of SA inhibited *SlCLH2* mRNA accumulation compared against non-treated samples. *SlCLH4* expression exhibited variable responses upon growth regulator application. Leaves of plants grown in the presence of MCP accumulate less, yet constant, amount of *SlCLH4* mRNA than controls. Upon ET application, *SlCLH4* expression decreased

Table 1
Evolutionary analysis of *CLH* and *PPH* sequences.

	Number of sequences	Number of codons	Mean *dN* ± SE	Mean *dS* ± SE	Mean Nc ± SD[a]	M0			M1a					2Δl (M1a–M0)[g]
						ω0[b]	p0[c]	lnl[d]	ω0	p0	ω1[e]	p1[f]	lnl	
All *CLHs*	38	234	0.330 ± 0.014	0.723 ± 0.010	51.14 ± 8.64	0.23984	1.00000	-16042.717743	0.17541	0.69088	1.00000	0.30912	-15781.792075	521.85*
Group I	13	281	0.186 ± 0.011	0.613 ± 0.015	50.08 ± 3,04	0.15071	1.00000	-5917.189525	0.09879	0.80370	1.00000	0.19630	-5845.329127	143.72*
Group II	16	269	0.325 ± 0.013	0.637 ± 0.013	55.97 ± 4.21	0.28053	1.00000	-8068.742702	0.14568	0.60939	1.00000	0.39061	-7912.028941	313.43*
Solanaceae Group I	4	278	0.140 ± 0.011	0.355 ± 0.023	53.46 ± 1.96	0.28452	1.00000	-2231.814979	0.18233	0.83215	1.00000	0.16785	-2225.767086	12.09*
Brassicaceae Group I	3	324	0.066 ± 0.050	0.323 ± 0.239	60.82 ± 0.31	0.21138	1.00000	-1936.781773	0.02253	0.73739	1.00000	0.26261	-1930.121126	13.32*
Solanaceae Group II	*4*	288	0.090 ± 0.009	0.348 ± 0.026	47.38 ±2.17	0.16221	1.00000	-2084.000701	0.14081	0.96064	1.00000	0.03936	-2082.982486	2.04
Brassicaceae Group II	3	317	0.053 ± 0.041	0.325 ± 0.270	55.57 ± 0.52	0.17562	1.00000	-1797.414114	0.09724	0.88243	1.00000	0.11757	-1794.771181	5.29
All *PPHs*	18	326	0.143 ± 0.009	0.635 ± 0.013	53.92 ± 2.42	0.12057	1.00000	-8204.934624	0.07911	0.86475	1.00000	0.13525	-8069.057688	271.75*
Solanaceae PPHs	3	478	0.054 ± 0.006	0.197 ± 0.017	50.72 ± 1.71	0.23623	1.00000	-2787.421353	0.17129	0.90511	1.00000	0.09489	-2786.327631	2.18
Brassicaceae PPHs	3	476	0.071 ± 0.019	0.313 ± 0.038	54.33 ± 1.15	0.23429	1.00000	-3047.214210	0.19376	0.93393	1.00000	0.06607	-3046.592305	1.24

[a] Nc: effective number of codons and the corresponding standard deviation (SD). No significant differences in codon usage were identified ($p < 0.01$). [b] ω0: ω estimates for the codons under purifying selection. [c] p0: estimated proportion of codons under purifying selection. [d] lnl: log likelihood of model. [e] ω1: ω estimates for the codons under neutral evolution. [f] p1: estimated proportion of codons under neutral evolution. [g] 2Δl (M1a–M0): the likelihood ratio statistics (2Δl) is approximated by the χ^2 distribution (degree of freedom = 1). Null hypotheses (M0) rejected is highlighted in dark gray and indicated with an asterisk in the 2Δl (M1a–M0) ($p < 0.01$). Null hypotheses (M0) accepted are highlighted in light gray.

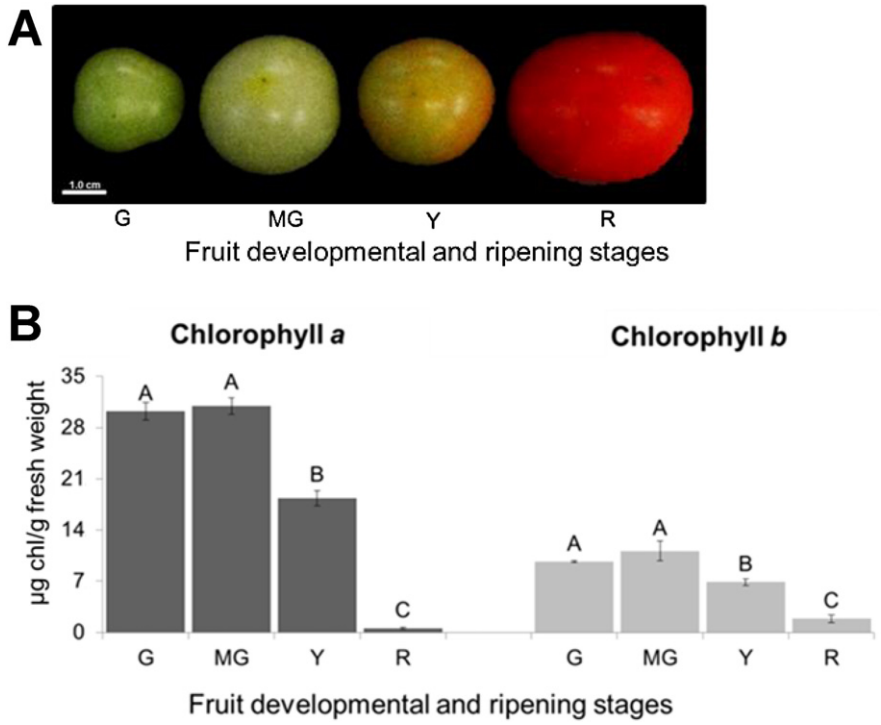

Fig. 4. Chlorophyll content during fruit development and ripening. (A) Phenotypic characteristics of the fruits. (B) Chlorophyll *a* and chlorophyll *b* content in fruits. Fruit pericarp material was sampled during natural development and ripening at four different stages: green (G), mature green (MG), yellow (Y) and ripe (R). Different letters indicate statistically significant values compared with the corresponding G stage ($p < 0.05$).

after 2 days of treatment and rapidly returned to basal levels. ABA and SA application inhibited *SlCLH4* mRNA accumulation, which decreased 76% and 90% after 4 days, respectively. Finally, *SlPPH* showed an expression profile that mirrored the Chl *a* content and *SlCLH1* expression pattern, suggesting its involvement in senescence-induced chlorophyll degradation.

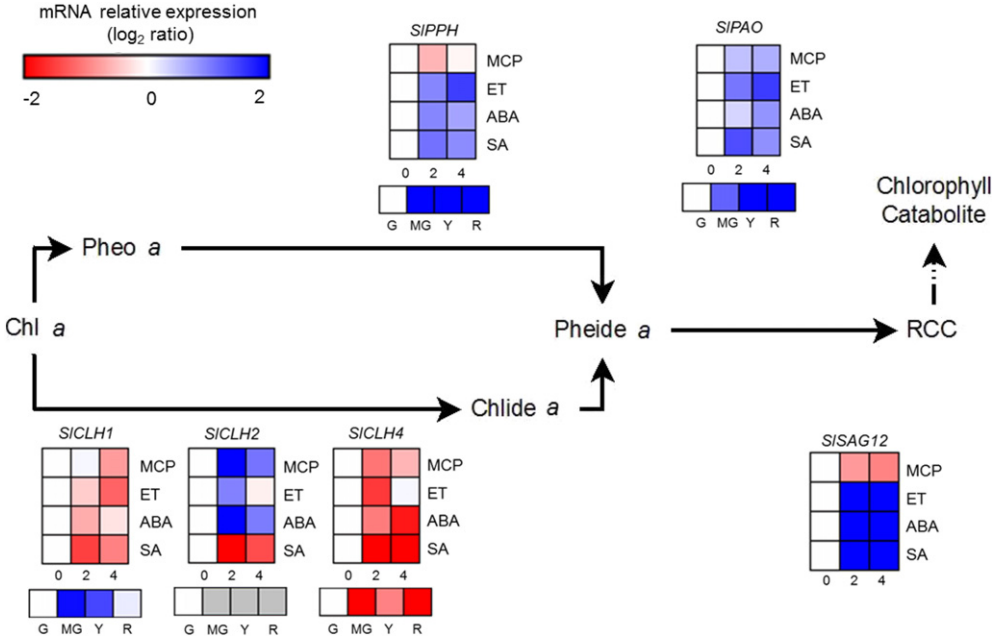

Fig. 5. Expression of the dephytylating enzyme-encoding genes in leaves and fruits. Schematic view of the Chl degradation pathway showing the relative expression profile of *SlCLH1*, *SlCLH2*, *SlCLH4* and *SlPPH* assayed by qPCR. Leaves were analyzed after 0, 2 or 4 days of treatment with 1-methylcyclopropene (MCP), ethylene (ET), abscisic acid (ABA) or salicylic acid (SA). Fruit transcript profiles were performed at green (G), mature green (MG), yellow (Y) and ripe (R) stages. *SlSAG12* and *SlPAO* were included as controls. Values represent means from at least three biological replicates. Mean relative expression was calculated from the means of two technical replicates and normalized against non-treated samples (day 0) or green fruits (G). Leaf expression data were expressed as the ratio between the treatment value and the corresponding untreated control. The expression values and the corresponding statistically significant differences ($p < 0.05$) between samples are detailed in Tables S4 and S5. Gray boxes denote not detected. Chl *a*, chlorophyll *a*; Pheo *a*, pheophytin *a*; Chlide *a*, chlorophyllide *a*; Pheide *a*, pheophorbide *a*; RCC, red chlorophyll catabolite; *CLH*, chlorophyllase; *PPH*, pheophytinase; *PAO*, pheophorbide *a* oxygenase; *SAG12*, senescence-induced marker gene.

Once tomato fruits are fully expanded at the MG stage, one of the most obvious visible changes is a modification of color resulting from the degradation of chlorophyll and the accumulation of carotenoid pigments. Indicative of the early onset of chlorophyll degradation, the *SlPPH* and *SlCLH1* showed a peak of expression at the MG stage, which decreased towards the R stage. In contrast, *SlCLH4* displayed a fluctuating expression profile with higher mRNA levels in the G and Y stages and lower amount of transcripts in the MG and R stages (Fig. 5, Table S5).

4. Discussion

Although the cytotoxic effects of Chl metabolism intermediates are well known, there are still many poorly understood steps in the Chl degradation pathway. Moreover, since most studies have focused on Chl breakdown during leaf senescence, knowledge of Chl degradation during fruit ripening is very limited (Hörtensteiner, 2013). We therefore performed a comparative study of both processes in *S. lycopersicum* focusing on the gene encoding dephytylating enzymes. A survey of the tomato genome (The Tomato Genome Consortium, 2012) revealed four *CLH-like* and a single *PPH-like* genes.

In silico prediction of subcellular localization suggested that, as described for the *A. thaliana* ortholog, SlPPH is located in the chloroplast (Schelbert et al., 2009). In agreement with the divergent data obtained from different experimental approaches (Azoulay-Shemer et al., 2008, 2011; Harpaz-Saad et al., 2007), for SlCLHs the protein sequence analyses were not conclusive with respect to organelle targeting. The phenetic analysis showed that, with the exception of *E. grandis* and *Oryza sativa*, the analyzed species had two or three copies of *CLH* genes. Interestingly, among the fourteen species examined, *Solanum tuberosum* and *S. lycopersicum* were the only examples with four *CLH*s, suggesting a lineage-specific duplication. In contrast, *PPH* was apparently present as a single copy gene. The existence of two groups of CLHs suggests functional diversification, and a selective constraint study revealed that different dephytylating-encoding genes are likely subjected to distinct selective pressures. Moreover, the differing expression profiles discussed below further suggests the existence of functional specificity. However, it is important to note that in *Citrus*, chlorophyllase is subjected to N- and C-terminal processing, so post-translational regulatory mechanisms may also participate in the regulation of enzyme activity (Azoulay-Shemer et al., 2011).

Our expression data indicate that SlPPH is the principal dephytylating enzyme acting during leaf senescence, as has been demonstrated for the ortholog in *A. thaliana* (Schelbert et al., 2009), and its expression coincides with Chl *a* catabolism. The levels of *SlCLH1* mRNA gradually decreased correlating with Chl amount during hormone-induced leaf senescence. The same behavior was observed for the *CLH* of *Ginkgo biloba* during autumnal yellowing (Tang et al., 2004) and *AtCLH2* along dark-induced senescence (Liao et al., 2007), which belong to the same group of *SlCLH1*. These results are indicative of Group II CLH involvement in the homeostasis of Chls in leaves, as was previously suggested by Tang et al. (2004). In contrast, *SlCLH2* and *SlCLH4* displayed variable expression patterns upon the tested stimuli. This is in agreement with all functional studies performed with Group I *CLH*s that have indicated responsiveness to external and hormonal stimuli, such as abscisic acid (ABA) (Gupta et al., 2012), methyl-jasmonate (Kariola et al., 2005; Schenk et al., 2007; Tsuchiya et al., 1999), wounding (Benedetti and Arruda, 2002; Kariola et al., 2005), pathogen elicitors (Kariola et al., 2005) and salicylic acid (Kariola et al., 2005). It is worth to remark the drastic reduction of *SlCLH2* and *SlCLH4* expression in response to SA, which after 2 days of treatment the mRNA levels dropped to 2% and 19%, respectively. The corresponding ortholog gene from *A. thaliana*, *AtCLH1*, has also shown to modulate SA signaling. During an SA-dependent defense response, cell damage causes Chl leaking. As a result of the phototoxic nature of this pigment, the delay of free Chl degradation by the *AtCLH1* transcriptional inhibition enhanced reactive oxygen species accumulation, which boosts defense response (Kariola et al., 2005).

Regarding *SlCLH3*, the absence of detectable levels of mRNA described here is in accordance with RNAseq public data available at Tomato Functional Genomic Database at Sol Genomics Network (http://solgenomics.net/) for *S. lycopersicum* cv. Heinz and *Solanum pimpinellifolium*. However, a comprehensive analysis of the gene sequence did not indicate any feature that could suggest that *SlCLH3* locus was a pseudogene.

The expression of the gene encoding the dephytylating enzymes during fruit degreening showed similar behavior from what was observed during leaf senescence. At the MG stage, when fruits have reached their maximum size and Chl content before the triggering of ET biosynthesis (Giovannoni, 2004), *SlCLH1* exhibited the highest levels of mRNA accumulation, which then decreased during ripening together with both Chl *a* and *b* levels. From G to MG stage, *SlPPH* expression increased over 40-fold. This expression pattern indicates that *SlPPH* and *SlCLH1* transcriptional regulation is ET-independent in fruits. The correlation of *SlCLH1* expression patterns with Chl content again indicates its involvement in pigment homeostasis. Additionally, *SlPPH* up-regulation demonstrates that Chl degradation during tomato degreening mostly depends on this enzyme. However, the transcriptional induction of *SlCLH1* observed in MG stage (2.5-fold) suggests a synergistic action of SlPPH and SlCLH1 on fruit Chl catabolism during chloroplast to chromoplast transition. Additionally, as observed in leaves, the expression of *SlCLH4* showed to be responsive to ABA displaying reduction of mRNA levels following ABA accumulation at late expansion (G) and early ripening (Y) phases (McAtee et al., 2013; Seymour et al., 2013), further underlining the responsiveness of Group I *CLH*s to phytohormones. However, in light of the extremely low expression level of *SlCLH4*, the role of Group I *CLH*s in tomato ripening is questionable.

The data presented here, together with previous studies, indicate three main physiological roles for the dephytylating enzymes. PPH acts as part of a multi-enzymatic complex during developmentally programed physiological processes such as leaf senescence and fruit ripening, and so experiences a high degree of selective constraint (Sakuraba et al., 2012, 2013). CLHs belonging to Group I respond to external and hormonal stimuli. Since this group of enzymes is under relaxed purifying selection, a certain degree of sequence variability may have helped the development of tailored defense response pathways according to the varying environment and pathogen pressures during the evolutionary history. Finally, CLHs belonging to Group II are involved in Chl homeostasis and phytol recycling in leaves and fruits, and are subjected to higher levels of purifying selection (Almeida et al., 2011; Ischebeck et al., 2006; Quadrana et al., 2013; Tang et al., 2004; Vavilin and Vermaas, 2007). In summary, an integrated analysis of the results obtained from the genomic, evolutionary and expression studies of tomato *PPH* and *CLH*-encoding genes, demonstrated that the different Chl dephytylation enzymes play specific roles in plant physiology and plant–environment interactions.

Supplementary data to this article can be found online at http://dx.doi.org/10.1016/j.gene.2014.05.051.

Conflict of interest

There are no conflict of interest.

Acknowledgments

BSL and JA were recipients of FAPESP fellowships and MR was funded by a fellowship from CNPq. This work was supported by FAPESP 2012-12531-8 (Brazil). The authors thank Rohm and Haas Company for generous donation of the 1-methylcyclopropene (SmartFresh®) used for the experiments.

References

Almeida, J., Quadrana, L., Asís, R., Setta, N., De Godoy, F., Bermúdez, L., Otaiza, S.N., Corrêa da Silva, J.V., Fernie, A.R., Carrari, F., Rossi, M., 2011. Genetic dissection of vitamin E biosynthesis in tomato. J. Exp. Bot. 62, 3781–3798.

Altschul, S.F., Gish, W., Miller, W., Myers, E.W., Lipman, D.J., 1990. Basic local alignment search tool. J. Mol. Biol. 215, 403–410.

Azoulay-Shemer, T., Harpaz-Saad, S., Belausov, E., Lovat, N., Krokhin, O., Spicer, V., Standing, K.G., Goldschmidt, E.E., Eyal, Y., 2008. Citrus chlorophyllase dynamics at ethylene-induced fruit color-break: a study of chlorophyllase expression, posttranslational processing kinetics, and in situ intracellular localization. Plant Physiol. 148, 108–118.

Azoulay-Shemer, T., Harpaz-Saad, S., Cohen-Peer, R., Mett, A., Spicer, V., Lovat, N., Krokhin, O., Brand, A., Gidoni, D., Standing, K.G., Goldschmidt, E.E., Eyal, Y., 2011. Dual N- and C-terminal processing of citrus chlorophyllase precursor within the plastid membranes leads to the mature enzyme. Plant Cell Physiol 52, 70–83.

Bannai, H., Tamada, Y., Maruyama, O., Nakai, K., Miyano, S., 2002. Extensive feature detection of N-terminal protein sorting signals. Bioinformatics 18, 298–305.

Barry, C.S., McQuinn, R.P., Chung, M.Y., Besuden, A., Giovannoni, J.J., 2008. Amino acid substitutions in homologs of the STAY-GREEN protein are responsible for the green-flesh and chlorophyll retainer mutations of tomato and pepper. Plant Physiol. 147, 179–187.

Benedetti, C.E., Arruda, P., 2002. Altering the expression of the chlorophyllase gene *ATHCOR1* in transgenic *Arabidopsis* caused changes in the chlorophyll-to-chlorophyllide ratio. Plant Physiol. 128, 1255–1263.

Benedetti, C.E., Costa, C.L., Turcinelli, S.R., Arruda, P., 1998. Differential expression of a novel gene in response to coronatine, methyl jasmonate, and wounding in the *coi1* mutant of *Arabidopsis*. Plant Physiol. 116, 1037–1042.

Blankenship, S.M., Dole, J.M., 2003. 1-Methylcyclopropene: a review. Postharvest Biol. Technol. 28, 1–25.

Blum, T., Briesemeister, S., Kohlbacher, O., 2009. MultiLoc2: integrating phylogeny and Gene Ontology terms improves subcellular protein localization prediction. BMC Bioinforma. 10, 274.

Briesemeister, S., Blum, T., Brady, S., Lam, Y., Kohlbacher, O., Shatkay, H., 2009. SherLoc2: a high-accuracy hybrid method for predicting subcellular localization of proteins. J. Proteome Res. 8, 5363–5366.

Büchert, A.M., Civello, P.M., Martínez, G., 2011. Chlorophyllase versus pheophytinase as candidates for chlorophyll dephytylation during senescence of broccoli. J. Plant Physiol. 168, 337–343.

Chou, K.C., Shen, H.B., 2010. Plant-mPLoc: a top-down strategy to augment the power for predicting plant protein subcellular localization. PLoS ONE 5, e11335.

Di Rienzo, J.A., 2009. Statistical Software for the Analysis of Experiments of Functional Genomics. RDNDA, Argentina, (http://sites.google.com/site/fgStatistics/).

Di Rienzo, J.A., Casanoves, F., Balzarini, M.G., Gonzalez, L., Tablada, M., Robledo, C.W., 2011. InfoStat Versión 2011. Grupo InfoStat, FCA, Universidad Nacional de Córdoba, Argentina, (http://www.infostat.com.ar).

Efrati, A., Eyal, Y., Ilan, P., 2005. Molecular mapping of the chlorophyll retainer (*cl*) mutation in pepper (*Capsicum* spp.) and screening for candidate genes using tomato ESTs homologous to structural genes of the chlorophyll catabolism pathway. Genome 48, 347–351.

Emanuelsson, O., Brunak, S., von Heijne, G., Nielsen, H., 2007. Locating proteins in the cell using TargetP, SignalP, and related tools. Nat. Protoc. 2, 953–971.

Giovannoni, J.J., 2004. Genetic regulation of fruit development and ripening. Plant Cell 16, 170–180.

Gupta, S., Gupta, S.M., Sane, A.P., Kumar, N., 2012. Chlorophyllase in *Piper betle* L. has a role in chlorophyll homeostasis and senescence dependent chlorophyll breakdown. Mol. Biol. Rep. 39, 7133–7142.

Harpaz-Saad, S., Azoulay, T., Arazi, T., Ben-Yaakov, E., Mett, A., Shiboleth, Y.M., Hörtensteiner, S., Goldschmidt, E.E., Eyal, Y., 2007. Chlorophyllase is a rate-limiting enzyme in chlorophyll catabolism and is posttranslationally regulated. Plant Cell 19, 1007–1022.

Hörtensteiner, S., 2006. Chlorophyll degradation during senescence. Annu. Rev. Plant Biol. 57, 55–77.

Hörtensteiner, S., 2013. Update on the biochemistry of chlorophyll breakdown. Plant Mol. Biol. 82, 505–517.

Hörtensteiner, S., Kräutler, B., 2011. Chlorophyll breakdown in higher plants. Biochim. Biophys. Acta 1807, 977–988.

Ischebeck, T., Zbierzak, A.M., Kanwischer, M., Dörmann, P., 2006. A salvage pathway for phytol metabolism in *Arabidopsis*. J. Biol. Chem. 281, 2470–2477.

Jacob-Wilk, D., Holland, D., Goldschmidt, E.E., Riov, J., Eyal, Y., 1999. Chlorophyll breakdown by chlorophyllase: isolation and functional expression of the *Chlase1* gene from ethylene-treated Citrus fruit and its regulation during development. Plant J. 20, 653–661.

Kariola, T., Brader, G., Li, J., 2005. Chlorophyllase 1, a damage control enzyme, affects the balance between defense pathways in plants. Plant Cell 17, 282–294.

Khan, M., Rozhon, W., Poppenberger, B., 2013. The role of hormones in the aging of plants — a mini-review. Gerontology. http://dx.doi.org/10.1159/000354334.

Liao, Y., An, K., Zhou, X., Chen, W., 2007. *AtCLH2*, a typical but possibly distinctive chlorophyllase gene in *Arabidopsis*. J. Integr. Plant Biol. 49, 531–539.

Lichtenthaler, H.K., 1987. Chlorophylls and carotenoids: pigments of photosynthetic biomembranes. Methods Enzymol. 148, 350–382.

Lim, P.O., Kim, H.J., Nam, H.G., 2007. Leaf senescence. Annu. Rev. Plant Biol. 58, 115–136.

McAtee, P., Karim, S., Schaffer, R., David, K., 2013. A dynamic interplay between phytohormones is required for fruit development, maturation, and ripening. Front. Plant Sci. 4, 79.

Murashige, T., Skoog, F., 1962. A revised medium for rapid growth and bioassays with tobacco tissue cultures. Physiol. Plant. 15, 473–497.

Nitsch, L., Kohen, W., Oplaat, C., Charnikhova, T., Cristescu, S., Michieli, P., Wolters-Artsa, M., Bouwmeesterb, H., Mariania, C., Vriezena, W.H., Rieua, I., 2012. ABA-deficiency results in reduced plant and fruit size in tomato. J. Plant Physiol. 169, 878–883.

Pfaffl, M.W., Horgan, G.W., Dempfle, L., 2002. Relative expression software tool (REST) for group-wise comparison and statistical analysis of relative expression results in real-time PCR. Nucleic Acids Res. 30, e36.

Pierleoni, A., Martelli, P.L., Fariselli, P., Casadio, R., 2006. BaCelLo: a balanced subcellular localization predictor. Bioinformatics 22, e408–e416.

Pino, L.E., Lombardi-Crestana, S., Azevedo, M.S., Scotton, D.C., Borgo, L., Quecini, V., Figueira, A., Peres, L.E.P., 2010. The *Rg1* allele as a valuable tool for genetic transformation of the tomato 'Micro-Tom' model system. Plant Methods 6, 23.

Pružinska, A., Tanner, G., Anders, I., Roca, M., Hörtensteiner, S., 2003. Chlorophyll breakdown: pheophorbide a oxygenase is a Rieske-type iron–sulfur protein, encoded by the accelerated cell death 1 gene. Proc. Natl. Acad. Sci. U. S. A. 100, 15259–15264.

Quadrana, L., Almeida, J., Otaiza, S.N., Duffy, T., Corrêa da Silva, J.V., de Godoy, F., Asís, R., Bermúdez, L., Fernie, A.R., Carrari, F., Rossi, M., 2013. Transcriptional regulation of tocopherol biosynthesis in tomato. Plant Mol. Biol. 81, 309–325.

Ruijter, J.M., Ramakers, C., Hoogaars, W.M., Karlen, Y., Bakker, O., van den Hoff, M.J., Moorman, A.F.M., 2009. Amplification efficiency: linking baseline and bias in the analysis of quantitative PCR data. Nucleic Acids Res. 37, e45.

Sakuraba, Y., Kim, Y.S., Yoo, S.C., Hörtensteiner, S., Paek, N.C., 2013. 7-Hydroxymethyl chlorophyll a reductase functions in metabolic channeling of chlorophyll breakdown intermediates during leaf senescence. Biochem. Biophys. Res. Commun. 430, 32–37.

Sakuraba, Y., Schelbert, S., Park, S.Y., Han, S.H., Lee, B.D., Andrès, C.B., Kessler, F., Hörtensteiner, S., Paek, N.C., 2012. STAY-GREEN and chlorophyll catabolic enzymes interact at light-harvesting complex II for chlorophyll detoxification during leaf senescence in *Arabidopsis*. Plant Cell 24, 507–518.

Schelbert, S., Aubry, S., Burla, B., Agne, B., Kessler, F., Krupinska, K., Hörtensteiner, S., 2009. Pheophytin pheophorbide hydrolase (pheophytinase) is involved in chlorophyll breakdown during leaf senescence in *Arabidopsis*. Plant Cell 21, 767–785.

Schenk, N., Schelbert, S., Kanwischer, M., Goldschmidt, E.E., Dörmann, P., Hörtensteiner, S., 2007. The chlorophyllases *AtCLH1* and *AtCLH2* are not essential for senescence-related chlorophyll breakdown in *Arabidopsis thaliana*. FEBS Lett. 581, 5517–5525.

Seymour, G.B., Østergaard, L., Chapman, N.H., Knapp, S., Martin, C., 2013. Fruit development and ripening. Annu. Rev. Plant Biol. 64, 219–241.

Tamura, K., Dudley, J., Nei, M., Kumar, S., 2007. MEGA4: Molecular Evolutionary Genetics Analysis (MEGA) software version 4.0. Mol. Biol. Evol. 24, 1596–1599.

Tang, L., Okazawa, A., Itoh, Y., Fukusaki, E., Kobayashi, A., 2004. Expression of chlorophyllase is not induced during autumnal yellowing in *Ginkgo biloba*. Z. Naturforsch. C 59, 415–420.

The Tomato Genome Consortium, 2012. The tomato genome sequence provides insights into fleshy fruit evolution. Nature 485, 635–641.

Tsuchiya, T., Ohta, H., Okawa, K., Iwamatsu, A., Shimada, H., Masuda, T., Takamiya, K., 1999. Cloning of chlorophyllase, the key enzyme in chlorophyll degradation: finding of a lipase motif and the induction by methyl jasmonate. Proc. Natl. Acad. Sci. U. S. A. 96, 15362–15367.

Vavilin, D., Vermaas, W., 2007. Continuous chlorophyll degradation accompanied by chlorophyllide and phytol reutilization for chlorophyll synthesis in *Synechocystis* sp. PCC 6803. Biochim. Biophys. Acta 1767, 920–929.

Weaver, L.M., Gan, S., Quirino, B., Amasino, R.M., 1998. A comparison of the expression patterns of several senescence-associated genes in response to stress and hormone treatment. Plant Mol. Biol. 37, 455–469.

Yang, Z., 2007. PAML 4: a program package for phylogenetic analysis by maximum likelihood. Mol. Biol. Evol. 24, 1586–1591.

Yu, C.S., Chen, Y.C., Lu, C.H., Hwang, J.K., 2006. Prediction of protein subcellular localization. Proteins 64, 643–651.